Inorganic Chemistry

Article

pubs.acs.org/IC

Synthesis, Crystal Structure, and Bonding Analysis of the Hypoelectronic Cubic Phase $Ca_5Pd_6Ge_6$

Isa Doverbratt,* Siméon Ponou,† Fei Wang, and Sven Lidin

Centre for Analysis and Synthesis, Lund University, P.O. Box 124, 22100 Lund, Sweden

Supporting Information

ABSTRACT: The title compound, $Ca_5Pd_6Ge_6$, was obtained during a systematic investigation of the Ca−Pd−Ge ternary phase diagram. The crystal structure was determined and refined from single-crystal X-ray diffraction data. It crystallizes in a new structure variant of the Y_4PdGa_{12}-type structure ($Im\bar{3}m$, a = 8.7764(4) Å) that features an arrangement of vertex-sharing body-centered cubes of calcium, $Ca@Ca_8$, with a hierarchical bcc network, interpenetrating a second (Pd_6Ge_6) network consisting of Ge_2 dumbbells surrounded by Pd in a strongly flattened octahedron with Pd(μ^2-η^2,η^4-Ge_2)-like motifs. These octahedra are condensed through the Pd to form a 3D open fcc network. Theoretical band structure calculations suggested that the compound is hypoelectronic with predominantly multicenter-type interatomic interactions involving all three elements and essentially a Hume−Rothery-like regime of electronic stabilization. The similar electronegativity between germanium and palladium atoms has a decisive impact on the bonding picture of the system.

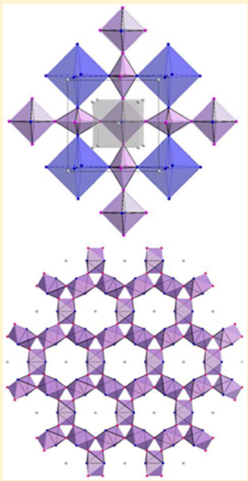

INTRODUCTION

Ternary compounds between noble metals and p-block (semi)metals and electropositive (active) metals such as alkali, alkaline-earth, and rare-earth metals tend to form extended networks[1−6] with significant charge transfer from the "isolated" electropositive active metal (no homonuclear direct contact) to the more electronegative noble metals and p-block atoms. In some peculiar cases, a closed -shell configuration is achieved for all main-group elements involved, through homonuclear two-center−two-electron (2c-2e) bonding, resulting in the so-called Zintl phases.[3−6] Nevertheless, the inclusion of transition metals goes along with increased difficulties to evaluate the extent of the charge transfer and to assign formal oxidation states, introducing additional challenges in rationalizing the chemical bonding by using the Zintl concept.[6−8] This conjecture is largely illustrated in our recent reports on the Ca-(Pt/Pd)-Ge systems. Examples include the Laves phase Ca_2Pd_3Ge,[9] which is best described as a Pd^0-stuffed Zintl phase, and the cluster compounds $Ca_{10}Pt_7Tt_3$ (Tt = Si, Ge),[10] featuring anionic Pt^{2-} atoms strongly bonded to Si or Ge through 2c-2e bonds. Moreover the analogous phases Ca_2Pt_2Ge and Ca_2Pd_2Ge are surprisingly nonisostructural as a result of the varying magnitude of (partial) charge transfer from Ca to either the (Pt_2Ge) or (Pd_2Ge) substructures.[11]

None of the phases in the Ca-(Pd/Pt)-(Si/Ge) ternary systems described so far show any mixing of the noble metal and the p-block metal, and the compounds are completely ordered. In the metal-rich section of the existing phase diagram, homonuclear Si−Si or Ge−Ge contacts are not observed due to the abundance of valence electrons, as predicted by the Zintl concept. Rather, the more or less strong Pt−Pt or Pd−Pd bonds are interesting examples of metal−metal bonds in their anionic form. In particular, the impact of the relativistic effects of their bonding characteristics can be nicely accessed when going from Pd to Pt.[12] In addition, the heteronuclear Pt/Pd−Si/Ge covalent bonds constitute another remarkable feature that seems to be decisive for the atomic ordering and structure stability. However, as we move our investigations close to the equiatomic region of the phase diagram, more Si−Si or Ge−Ge bonds are expected to form, as the average valence electron per atom diminishes. In the title compound, $Ca_5Pd_6Ge_6$, in which a transition of bond types from localized to delocalized interactions is suggested from the analysis of the bonding picture, we could identify structural motifs that are unprecedented in intermetallic chemistry. We report herein on the synthesis and structural characterization by X-ray diffraction studies of the novel cubic structure of $Ca_5Pd_6Ge_6$, as well as insight into the bonding characteristics with the help of first-principles theoretical band structure calculations.

EXPERIMENTAL SECTION

Synthesis. The compound was prepared with molar ratios 1:1:1 of the elements (Ca: ABCR, granular 99.99%; Pd: American Elements, pieces 99%; Ge: ABCR, powder 99.99%). All manipulations of the samples were performed in an argon-filled glovebox. The mixtures of

Received: July 9, 2015
Published: September 1, 2015

DOI: 10.1021/acs.inorgchem.5b01528
Inorg. Chem. 2015, 54, 9098−9104

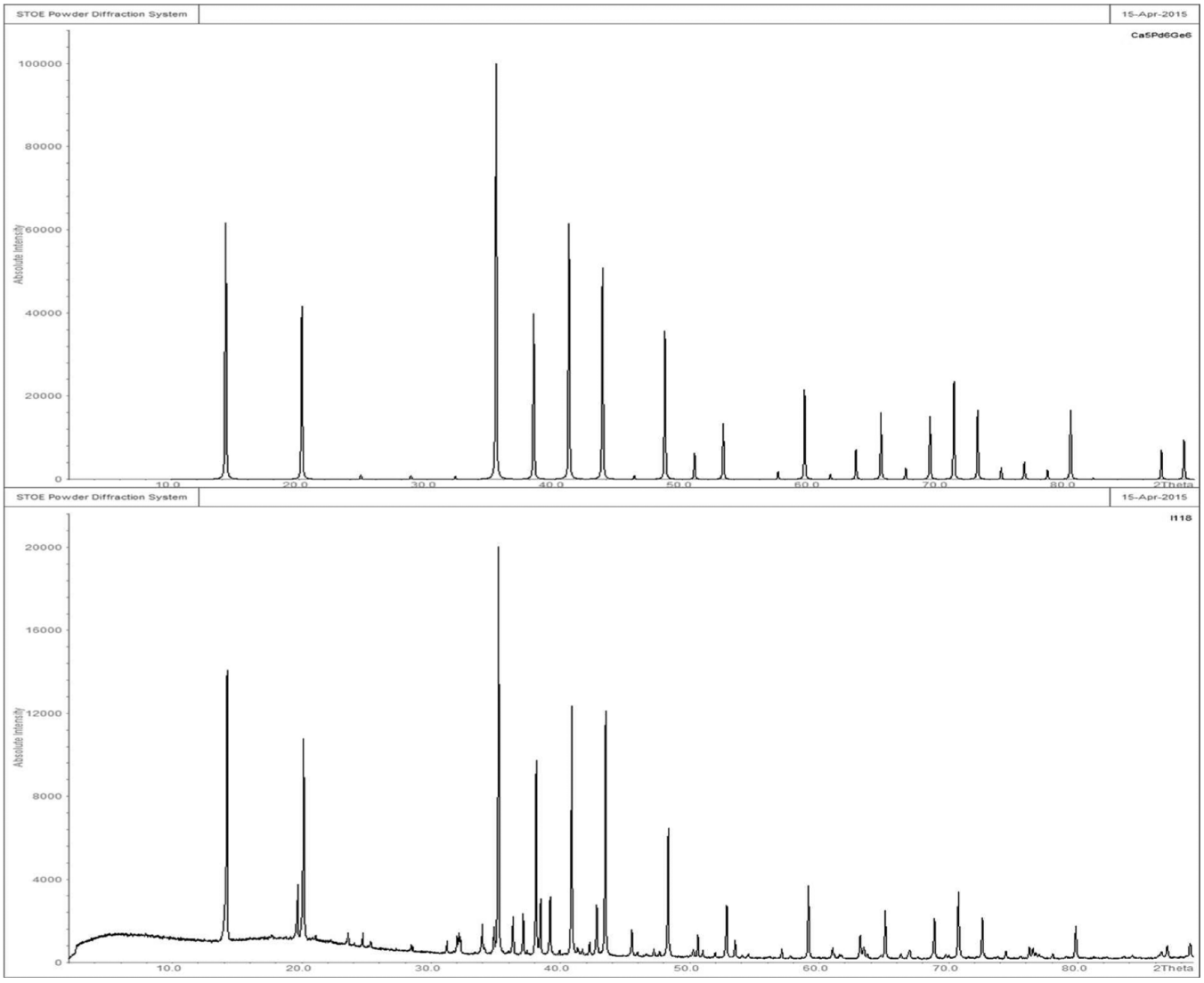

Figure 1. Comparison between powder pattern simulated from single-crystal data (top) and powder pattern of the product yielded from a synthesis with a 1:1:1 composition (bottom).

the elements were loaded in a niobium ampule and sealed by arc-melting. The ampule was enclosed in an evacuated Schlenk tube and heated in a tubular furnace up to 1273 K for 24 h, then annealed at 1223 K for 2 days and cooled to room temperature (1 °C/min). The title compound was obtained as a major phase, revealed by powder diffraction analysis, but a single crystal of the title compound could not be found. A single crystal of the title compound was however obtained from a synthesis prepared with the molar ratios 3:2:3. This sample was heated in a tubular furnace up to 1273 K, then annealed at 1223 K for 2 days and slowly cooled to room temperature (0.1 °C/min), yielding a sample containing several other compounds.

Structural Determination. A small dark metallic irregular crystal was fixed to a glass fiber using Epoxy glue, and the single-crystal data were collected at room temperature on an Oxford Diffraction Xcalibur EOS CCD diffractometer with graphite-monochromated Mo Kα radiation (λ = 0.710 73 Å) operated at 50 kV and 40 mA, with a detector distance of 50 mm, 10 s exposure time, and θ_{max} = 28.8°. The Oxford CrysAlis RED software was used for data processing, including an analytical absorption correction.[13] The data collection included 2294 frames from 14 ω-scans with 0.5°/frame scan width. Structural solution was accomplished using charge flipping as implemented in Superflip.[14] All refinements were performed using the JANA2006 software.[16] Further details on the crystal structure may be obtained from Fachinformationszentrum Karlsruhe, 76344 Eggenstein-Leopold-shafen, Germany (fax: (+49)7247-808-666; e-mail: crysdata@fiz-karlsruhe.de, http://.fiz-karlsruhe.de/request_for_deposited_data.html) on quoting the CSD number 429696.

EDX Analysis. The single crystal used in the X-ray experiment was analyzed by energy dispersive X-ray spectroscopy (EDX) using a field emission scanning electron microscope (JSM-6700F) equipped with an energy dispersive X-ray spectrometer (INCA-sight, Oxford Instruments, U.K.). Elemental Co was used as standard, and corrections for atomic number, absorption, and fluorescence were applied. The analysis confirmed the presence of all three elements, but the indicated atomic ratio Ca:Pd:Ge = 19:66:15 is not in agreement with the composition from single-crystal diffraction data (29:35:35).

X-ray Powder Diffraction. Diffraction patterns of the samples were recorded with a STOE X-ray powder diffractometer over 2θ ranges 2−90° with Cu Kα radiation (see Supporting Information). The samples were analyzed prior to and after exposure to air and showed that some of the phases present are air sensitive. The powder diffraction shows that the title compound is a minority phase in the sample yielding the single crystal used in the study.[15] This is not surprising given that the system contains a number of phases close to equiatomic 1:1:1 composition, Ca_2Pd_2Ge, $Ca_4Pd_4Ge_3$ ($Nd_4Rh_4Ge_3$-type), Ca_2Pd_3Ge (Mg_2Ni_3Si-type), and Ca_2PdGe_3 (Ce_2CoSi_3-type). Supporting that the composition obtained from single-crystal X-ray diffraction indeed is correct, we have observed this compound as a

DOI: 10.1021/acs.inorgchem.5b01528
Inorg. Chem. 2015, 54, 9098−9104

major phase in the powder pattern from a synthesis with a 1:1:1 composition (Figure 1). The single crystal of the compound has been handled in air for a long period of time and does not decompose on exposure.

Theoretical Calculations. The electronic structure and the chemical bonding of $Ca_5Pd_6Ge_6$ were investigated on the basis of the DFT approach and the linear muffin-tin orbital (LMTO) method in the atomic sphere approximation (ASA) using the tight-binding (TB) program LMTO-ASA.[17] The exchange correlation potential was parametrized according to Barth and Hedin.[18] The radii of the muffin-tin spheres were determined by an automatic procedure subject to a 16% overlap restriction,[19] and no additional empty spheres were necessary. The *k*-space integration was performed by the tetrahedron method, and the basis set employed was Ca-4s/(4p)/3d, Ge-4s/4p/(3d), and Pd-5s/5p/4d (down-folded orbitals in parentheses). The crystal orbital Hamilton population (COHP)[20] was used for the analysis of the relative bond strength. The Fermi level in all figures is set to zero, and the COHP diagrams are drawn by reversing their values with respect to the energy scale (i.e., COHP vs E). This is done so that the calculated peak values are negative for antibonding and positive for bonding interactions. The valence electron density map was calculated for $Ca_5Pd_6Ge_6$ with the ABINIT code.[21−23] We employed the norm-conserving pseudopotentials with the Perdew−Burke−Ernzerhof generalized gradient approximation.[24,25] The mesh sampling the first Brillouin zone is a 7 × 7 × 7. We set the energy cutoff of the plane wave basis set at 313.7 eV and adopted the Methfessel and Paxton occupational smearing scheme[26] (smearing energy 0.1 eV) to facilitate the self-consistent convergence.

Table 1. Crystallographic Data and Refinement Parameters for $Ca_5Pd_6Ge_6$

chemical formula	$Ca_5Pd_6Ge_6$
fw	1274.4 g·mol^{-1}
temp	293 K
wavelength	0.710 73 Å
data collection	Oxford Diffraction Xcalibur EOS
cryst syst	cubic
space group (no.)	$Im\bar{3}m$ (no. 229)
unit cell dimens	a = 8.7764(4) Å
volume	676.00(5) Å^3
Z	2
calcd density	6.255 g·cm^{-3}
absorp coeff	22.76 mm^{-1}
absorp corr	CrysAlis RED (analytical)
F(000)	1136
cryst size	0.06 × 0.03 × 0.01 mm^3
cryst color, θ range	dark gray, 3.28−28.79°
index ranges	$-11 \le h \le 11$; $-11 \le k \le 11$; $-11 \le l \le 11$
reflns collected	7896
indep reflns	112 (R_{int} = 0.090)
reflns with $I \ge 3\sigma(I)$	110
params	10
GOF on F^2	1.80
final R indices [$I > 3\sigma(I)$]	R_1 = 0.0158; wR_2 = 0.0476
R indices (all data)	R_1 = 0.0160; wR_2 = 0.0478
refinement method	full-matrix least-squares on F^2
extinction coefficient (×10^3)	490(40)
largest diff peak and hole	0.95 and −1.45 e Å^{-3}
weighting scheme	$w = 1/(\sigma^2(I) + 0.0004I^2)$

Table 2. Atomic Coordinates and Equivalent Isotropic Displacement Parameters (U_{eq})

atom	Wyckoff site	x	y	z	U_{eq} (Å^2)
Ca1	2*a*	0	0	0	0.0102(5)
Ca2	8*c*	1/4	1/4	1/4	0.0106(3)
Pd	12*d*	1/2	1/4	0	0.00884(19)
Ge	12*e*	0.34880(9)	0	0	0.0085(2)

RESULTS AND DISCUSSION

Structural solution and refinement were unproblematic, but elemental analysis (EDX 19:66:15) did not agree with the composition obtained from single-crystal X-ray diffraction (29:35:35). To ensure that this discrepancy is not the result of a simple mix-up, the crystal was remounted and data were recollected, confirming that the specimens used for EDX analysis and X-ray diffraction are identical. Attempts to change the nature of the occupied sites in the model were unsuccessful. In principle, a model where the Ge in site 12*e* is replaced by about 50% Pd and Ca in position 2*a* is fully replaced by Pd would not be too far off the EDX composition ($Ca_{20}Pd_{50}Ge_{15}$ = $Ca_{4,(8c)}Pd_{1,(2a)}Pd_{6,(12d)}Ge_{(6-x,(12e))}Pd_{x,(12e)}$, x = 3), but even this drastic change does not account for the discrepancy in the Pd content. Thus, the only plausible explanation we can find for the mismatch between the refined and EDX-determined composition is that the crystal is covered with a thin layer of Pd, which the electron beam, used in EDX, could not penetrate enough to get a proper analysis of the bulk crystal.

Structure and Crystal Chemistry. A description of the compound can start from assuming a Zintl-type behavior where the electronegative Pd and Ge form a covalently bonded three-dimensional anionic network, $[Pd_6Ge_6]^{10-}$, with Ca^{2+} as the counterion (Figure 2). The most striking feature of this structure is the vertex-sharing body-centered cubes of Ca (Wyckoff positions 2*a* and 8*c*) (Figure 3), and to our knowledge $Ca_5Pd_6Ge_6$ is the first ordered compound featuring this unusual $Ca@Ca_8$ unit, although it is observed in the alkaline earth nitride borates $(AE)_2(BN_2)_3$, but with vacancies.[27]

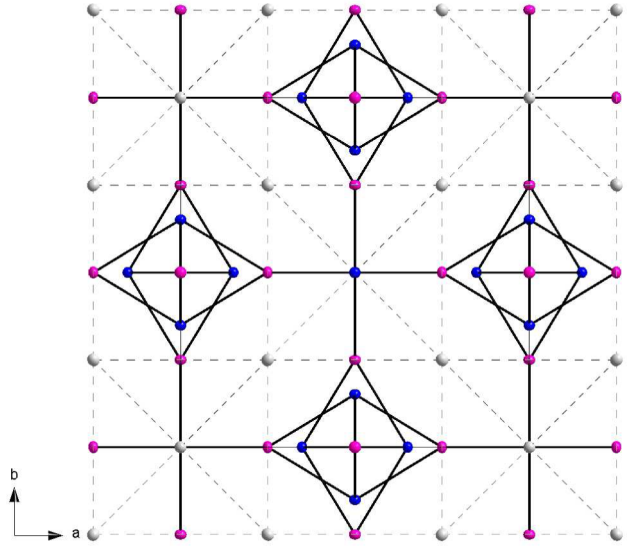

Figure 2. Structure of $Ca_5Pd_6Ge_6$ emphasizing the Pd_6Ge_6 substructure. Ca, gray; Pd, pink; Ge, blue. Displacement ellipsoids are drawn at the 50% probability level.

DOI: 10.1021/acs.inorgchem.5b01528
Inorg. Chem. 2015, 54, 9098−9104

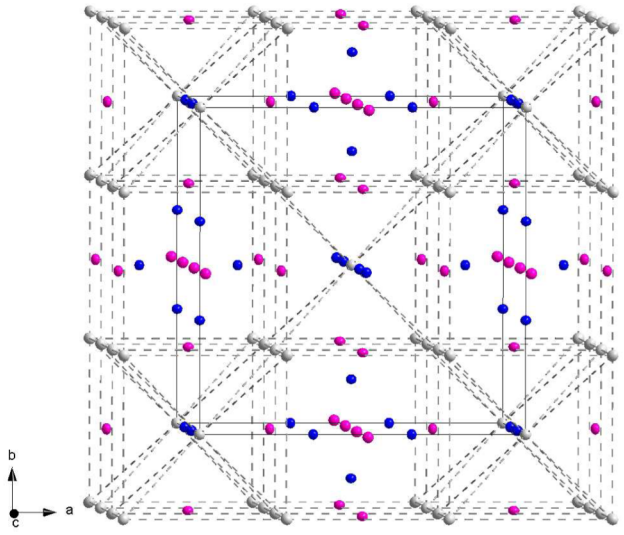

Figure 3. Perspective view of the $Ca_5Pd_6Ge_6$ structure showing the $Ca@Ca_8$ cubes in a fractal-like body-centered array. Ca, gray; Pd, pink; Ge, blue. Displacement ellipsoids are drawn at the 50% probability level.

Germanium atoms form dumbbells that are coordinating four Pd atoms, resulting in the corner-sharing flattened octahedra, which can be described as a $Pd(\mu^2\text{-}\eta^2,\eta^4\text{-}Ge_2)$-like motif, building the three-dimensional network. Ca1 (2*a*) is octahedrally surrounded by six Ge and has a cubic arrangement of eight Ca2 (8*c*), together forming a cuboctahedron. Ca2 forms a distorted cuboctahedron with six Pd (in a plane) and six Ge (Figure 4). There are two known coloring variant structure types closely resembling the title compound, having essentially the same geometrical arrangement of atoms and crystallizing in the same cubic space group $Im\bar{3}m$. These are $U_4Re_7Si_6$ and Y_4PdGa_{12}.[28] In the former, a Re_6Si_6 network interpenetrates with an arrangement of Re-centered, vertex-sharing $Re@U_8$ cubes, while Y_4PdGa_{12} features Pd-centered Y-cubes, $Pd@Y_8$, in a network of pure Ga atoms.

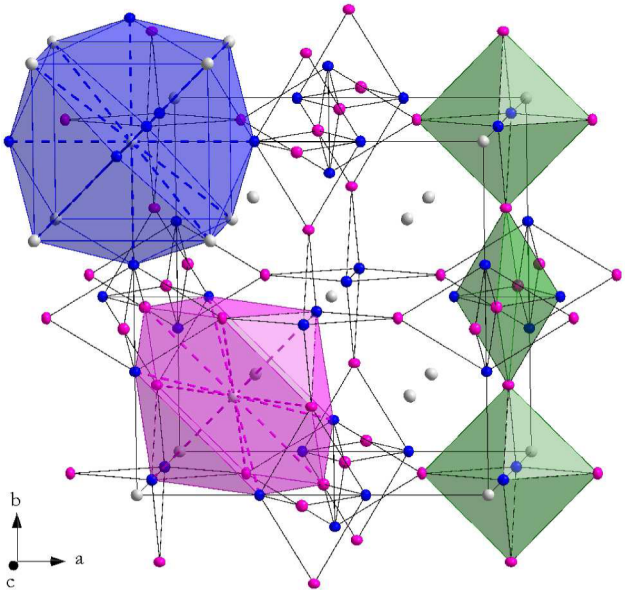

Figure 4. Anionic network formed by corner-sharing $\{Pd_6Ge_6\}$ flattened octahedra (green) and the Ca1 (2*a*) cuboctahedra (blue) and Ca2 (8*c*) distorted cuboctahedra (magenta).

The main difference is the element occupying the 2*a* position, the center of the alkaline-earth or rare-earth or actinoid cube. In the title compound this is Ca; in the two previously known examples it is a transition metal. It is notable that in another representative of this structure type, $Y_4Mn_{1-y}Ga_{12-x}Ge_x$,[29] the Mn deficiency is coupled to the Ge content so that upon increase of the Ge content, the Mn content also increases, hinting at an electronic stabilization mechanism in which the rare-earth Y atoms, forming the cubes, are donating electrons both to the Ga/Ge network and to the Mn in the 2*a* position.

The Pd_6Ge_6 network forms channels along the body diagonal ($^1/_2$ $^1/_2$ $^1/_2$) that are filled with linear Ca with a distance of 3.80 Å. The channels resemble those found in zeolites (Figure 5).

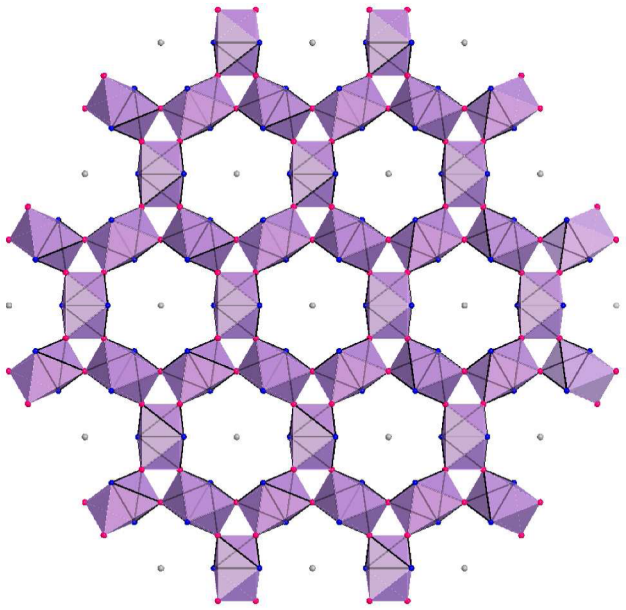

Figure 5. Zeolite-like channels ($^1/_2$ $^1/_2$ $^1/_2$ direction) formed by the Pd_6Ge_6 network filled with a linear Ca^{2+}arrangement. Thermal ellipsoids are drawn at the 50% probability level.

Bonding and Electronic Structure. To count the electrons in the title compounds, as the first step to understand the nature of the chemical bonding, we can use the Zintl–Klemm concept.[4] As there is one Ge–Ge bond (2.654 Å) in $Ca_5Pd_6Ge_6$, to a first approximation, this Ge atom require three extra electrons to complete its octet. Exaggerating the ionicity of the Ca and Pd interactions, the $Ca_5Pd_6Ge_6$ formula (assuming monovalent Pd) can be then broken down as $(Ca^{2+})_5(Pd^{+})_6(Ge^{3-})_6(-2e^{-})$, resulting in a two-electron shortage. The pairing of formally monovalent Pd species has been observed in carbonylation catalysts, but here the Pd atoms are relatively distant from each other, with a Pd–Pd distance of 3.103 Å, similar to the Ca–Pd distance. Alternatively, assuming divalent Pd will give $(Ca^{2+})_5(Pd^{2+})_6(Ge^{3-})_6(4e^{-})$. The four extra electrons are not compatible with the assumed covalent bonding within the Ge_2 dumbbells. The Ge–Ge bond distance of 2.654 Å is longer than the sum of atomic or covalent radii (2.40–2.50 Å),[30,31] and this can hardly be considered a pure 2c-2e bond. For comparison d_{Ge-Ge} = 2.529(3) Å for Ge_2 dumbbells in Ca_7Ge_6 in which partial π-bonding is assumed.[32]

DOI: 10.1021/acs.inorgchem.5b01528
Inorg. Chem. 2015, 54, 9098–9104

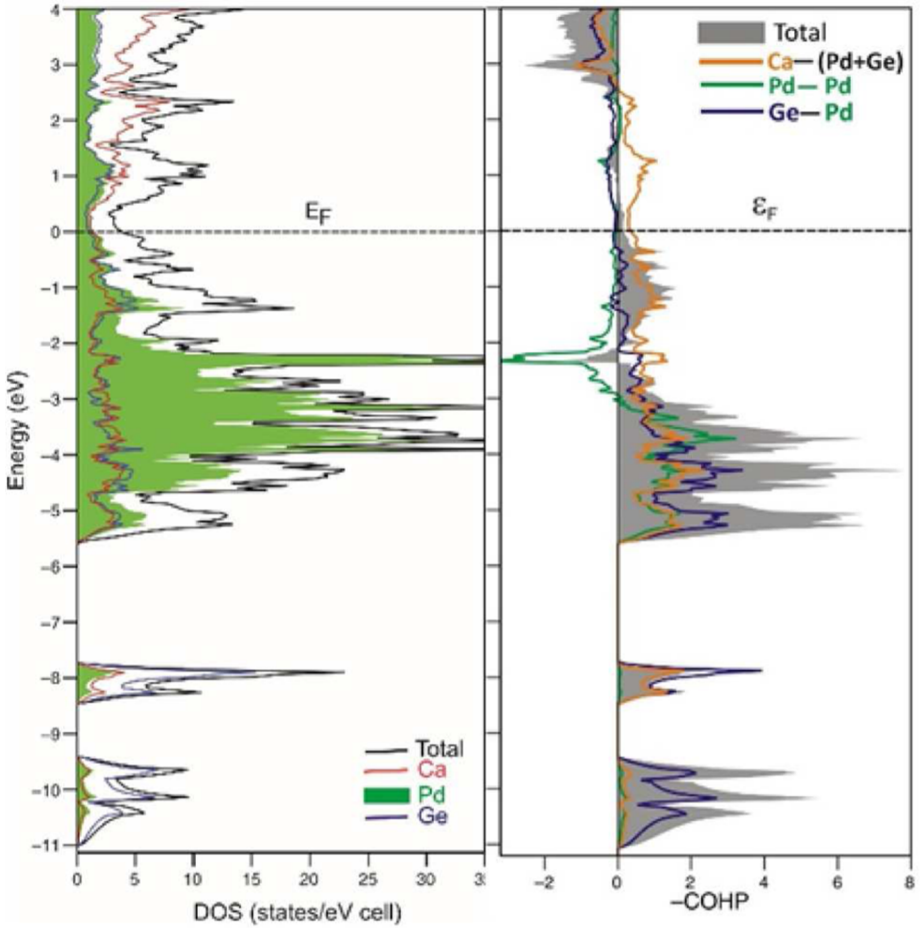

Figure 6. Density of state (DOS) plots with atomic projections and COHP curves for selected interactions in $Ca_5Pd_6Ge_6$ as obtained from LDA.

This conjecture may be applied also to $CaPd_2Ge_2$ ($ThCr_2Si_2$ type),[33] in which the Ge_2 pairs have a short Ge−Ge distance of 2.469 Å and interact with Pd atoms at 2.506 Å, quite similar to the Pd−Ge distance in the title compound. In that phase, the short Ge−Ge distance is more consistent with partial π-bond formation and is in contradiction with the simplified ionic formulation $Ca^{2+}(Pd^{2+})_2(Ge^{3-})_2$. To account for the relatively short Ge−Ge bond distance, the alternative formulation $Ca^{2+}(Pd_2)^{2+}(Ge{=}Ge)^{4-}$ with a double-bonded Ge_2 pair, or something halfway between, i.e., resonant-like $Ca^{2+}(Pd^{2+})_2(Ge^{3-})_2 \leftrightarrow Ca^{2+}(Pd_2)^{2+}(Ge{=}Ge)^{4-}$, seems to be more appropriate for $CaPd_2Ge_2$. Having this is mind, a compromise toward charge-balancing in the title compound may be to consider mixed or intermediate valence for Pd, even though only one Pd position is observed in the crystal, i.e., $(Ca^{2+})_5(Pd_6)^{8+}(Ge^{3-})_6$, but this would not explain the quite long Ge−Ge distance, which is more consistent with a fractional bond, typical of a delocalized multicenter bonded system. Assuming the Ge−Ge distance as nonbonding gives $(Ca^{2+})_5(Pd^{2+})_6(Ge^{4-})_6(2h^+)$, which is two-electron deficient (h^+ denotes a missing (hole) electron donor). Hence, by using an adaptation of the Wade−Mingos rules to condensed deltahedra,[34,35] an isolated $\{Pd_4Ge_2\}$ octahedron requires 26 valence electrons for seven bonding and six nonbonding (lone pairs) orbitals. As these octahedra condensed to form the 3D network, four out of the six lone pair orbitals create skeletal orbitals for fused octahedra; three of these remain bonding, giving 24 bonding orbitals for two $(Pd_{4/2}Ge_2)_3$ octahedra, meaning 48 valence electrons. Twenty-four and 10 valence electrons are provided by Ge and Ca atoms, respectively, and by assuming Pd^{2+}, the system is again two electrons short per formula unit. Apparently, fractional Ge−Ge bonding should be assumed as a result of the electron shortage.

Tight-binding linear-muffin-tin-orbital (TB-LMTO-ASA) electronic structure calculations using local density approximation (LDA) were carried out for the 94 valence electron phase $Ca_5Pd_6Ge_6$ to investigate the structure-directing forces as well as chemical bonding in this intricate phase. The calculated total and partial density of state (DOS) curves and the crystal orbital Hamilton populations for selected bonds are represented in Figure 6. The COHPs were integrated up to the Fermi level (ICOHP) for the Pd−Ge (−ICOHP = 1.83 eV/bond), Ge−Ge (−ICOHP = 1.49 eV/bond), and Pd−Pd (−ICOHP = 0.47 eV/bond) bonds. As shown in Figure 6, the Fermi level is at the edge of a pseudogap, suggesting that $Ca_5Pd_6Ge_6$ is very close to being charge-balanced with a slight electron deficiency. The nonzero DOS at the Fermi level (E_F) is a prediction of metallic properties, consistent with the color of the crystal, dark gray and lustrous. The bands at the Fermi level are mainly from Ca-3d, Pd-4d, and Ge-4p orbitals with almost identical contribution. Near the E_F, a strong mixing among Ca, Pd, and Ge states is observed, meaning that all atoms participate in covalent-type interactions, and the oversimplification of classical Zintl compounds is not applicable in this system.

DOI: 10.1021/acs.inorgchem.5b01528
Inorg. Chem. 2015, 54, 9098−9104

The COHP analysis of the interatomic interactions within the anionic $\{Pd_6Ge_6\}$ network indicates that those are nearly optimized and slightly antibonding around E_F. The Ca−Pd and Ca−Ge bonds remain bonding even above E_F, so that the overall interactions of the system show some residual unoccupied bonding states. Apparently the system will become electronically stabilized at 0.35 eV above E_F, by a combination of "anion−anion" and "cation−anion" interactions. Thus, with the pseudogap having its lower bound situated at 95 valence electrons, it suggests that the compound may be only one electron short per formula unit, with a Hume−Rothery-like regime of stabilization, with the bonding in the system being predominantly multicenter and delocalized.[36,37] Hence, the compound is only slightly off an optimum electronic stabilization of the electron-poor system with substantial contribution of Ca atoms to the bonding. Thus, if one considers the electronegativity of the elements (in the Pauling scale)[31] [χCa: 1.0, χPd: 2.20, and χGe: 2.01], Pd is more electronegative than Ge (albeit quite similar), and this is consistent with covalent Pd−Ge interactions observed as the strongest in the structure as compared to weaker Ge−Ge bonds according to bond distances and calculated −ICOHP values. From the calculated average −ICOHP value of Ca−Pd (0.57 eV/bond), Ca−Ge (0.65 eV/bond), and Pd−Pd (0.47 eV/bond), indicating weaker secondary interactions, we can conclude that the atomic ordering is mainly driven by the optimization of stronger Pd−Ge and Ge−Ge interactions that have stronger contribution to the overall system stability.[38] Nevertheless, the total Ca−Ge/Pd "cation−anion" interactions represent 34% of the total ICOHP calculated for the cubic $Ca_5Pd_6Ge_6$, and Ca cannot be regarded as a mere electron donor. This is probably because the Ge atoms are not electronegative enough to oxidize Pd atoms, and a formally closed-shell configuration is not achievable through the electrons donated by Ca. Therefore, the system bonding picture becomes more delocalized to accommodate the electron shortage. To further characterize the bonding in this system, the analysis of the charge calculated by pseudopotential method was also conducted.

The charge density plot (Figure 7) reveals that Ca atoms are approximately cationic: valence electrons are depleted around them. The electron-rich region defined by the isosurface encloses Pd and Ge atoms and also all the Pd−Ge heteroatomic connections. By contrast, the isosurface does not connect Ge with Ge, or Pd with Pd. Therefore, the heteroatomic Pd−Ge bonding is stronger than the homoatomic Ge−Ge and Pd−Pd bonding. This is in good agreement with the −ICOHP calculated with LMTO, which is highest for Pd−Ge bonding.

The isosurface plot also explains why the Zintl−Klemm formalism cannot be successfully applied to $Ca_5Pd_6Ge_6$. The distribution of valence electrons cannot be described by a collection of isolated and localized two-centered bonding or cluster bonding. Instead, the valence electrons smear over the whole Pd_6Ge_6 anionic network. In other words, valence electrons are only partially localized. They are enriched around Pd and Ge but still highly delocalized within the Pd_6Ge_6 anionic network. With such a large deviation from the localized bonding picture, the Zintl−Klemm formalism does not apply well. The delocalization of valence electrons also explains the poor metal feature of $Ca_5Pd_6Ge_6$ and the shallow pseudogap close to the E_F in its electronic structure.

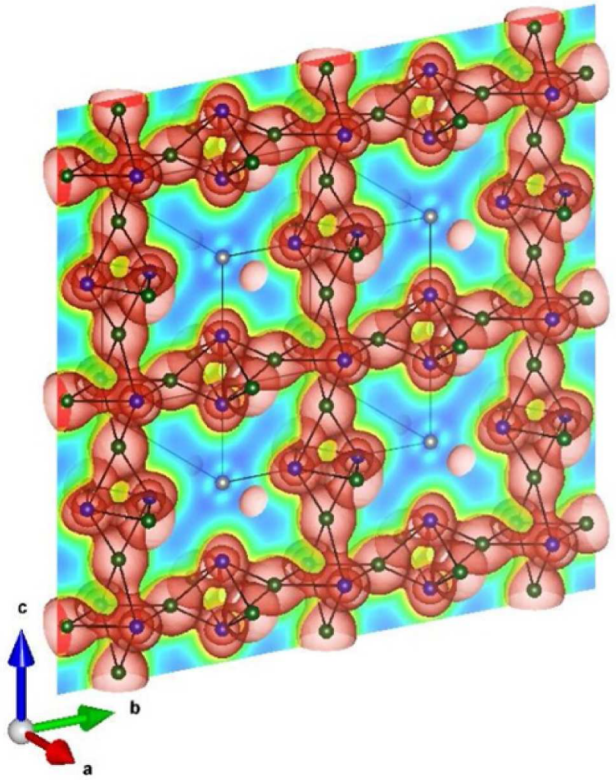

Figure 7. Valence electron density map of $Ca_5Pd_6Ge_6$: the red isosurface is drawn at 0.052 electron/Bohr^3, and the color-coded map is drawn in the (100) plane. Ca, gray; Pd, green; Ge, blue.

CONCLUSION

During our investigation of the Ca−Pd−Ge ternary system, $Ca_5Pd_6Ge_6$ was discovered. It is a new structure variant of the Y_4PdGa_{12}-type structure with a cubic structure showing intriguing structural and electronic features. It is best characterized as a polar intermetallic compound with metallic properties. In contrast to most molecular and simple semiconductor materials a closed-shell states is not achieved in the class of polar intermetallic compounds, resulting in the lack of simple valence rules to describe their bonding picture. Ternary phases between germanium, electropositive s-block metals, and noble metals such as Pd (or Ag and Pt) seem to generally result in (nearly) electronic stabilization by a complex "syncretism" between the Zintl concept and the Hume−Rothery mechanism, involving a significant charge transfer from the s-block metal Ca to the "anionic" substructure (Pd_6Ge_6). This results in multicenter delocalized bonding but, yet still substantial contribution of the Ca atoms to the system bonding. A complete atomic ordering is observed and is driven by the strongest Pd−Ge bonds, along with relatively weak Ge−Ge homonuclear interactions that are typically fractional bonds.[38] Remarkably, the weaker Pd−Pd bonding is also decisive to the system electronic stability through its enhanced ability to adjust the valence bond order to both the valence electron count and the extent of the charge transfer in order to foster the optimal achievable electronic stability for the system.

DOI: 10.1021/acs.inorgchem.5b01528
Inorg. Chem. 2015, 54, 9098−9104

■ ASSOCIATED CONTENT

Supporting Information

The Supporting Information is available free of charge on the ACS Publications website at DOI: 10.1021/acs.inorgchem.5b01528.

Single-crystal data in CIF format (CIF)
Powder diffraction data (PDF)

■ AUTHOR INFORMATION

Corresponding Author

*E-mail: isa.doverbratt@chem.lu.se.

Present Address

†(S.P.) Department of Chemistry, Iowa State University, 1605 Gilman Hall, Ames, Iowa 50011, United States.

Author Contributions

The manuscript was written through contributions of all authors. All authors have given approval to the final version of the manuscript.

Funding

We acknowledge the financial support of the Swedish National Research Council, VR.

Notes

The authors declare no competing financial interest.

■ REFERENCES

(1) (a) Corbett, J. D. *Inorg. Chem.* **2010**, *49*, 13−28. (b) Corbett, J. D. *Chem. Rev.* **1985**, *85*, 383−397.
(2) Corbett, J. D. In *Inorganic Chemistry in Focus II*; Meyer, G.; Naumann, D.; Wesemann, L., Eds.; Wiley-VCF: Weinheim, Germany, 2005; Vol. 2, Chapter 8.
(3) Nesper, R. *Angew. Chem.* **1991**, *103*, 805−834; *Angew. Chem., Int. Ed. Engl.* **1991**, *30*, 789−817.
(4) Schäfer, H.; Eisenmann, B.; Müller, W. *Angew. Chem., Int. Ed. Engl.* **1973**, *12*, 694.
(5) Nesper, R. *Prog. Solid State Chem.* **1990**, *20*, 1.
(6) *Chemistry, Structure, and Bonding of Zintl Phases and Ions*; Kauzlarich, S. M., Ed.; VCH: Weinheim, Germany, 1996.
(7) Kauzlarich, S. M.; Brown, S. R.; Snyder, G. J. *Dalton Trans.* **2007**, *21*, 2099−2107.
(8) (a) Whangbo, M.-H.; Lee, C.; Köhler, J. *Angew. Chem., Int. Ed.* **2006**, *45*, 7465. (b) Köhler, J.; Whangbo, M.-H. *Solid State Sci.* **2008**, *10*, 444. (c) Köhler, J.; Whangbo, M.-H. *Chem. Mater.* **2008**, *20*, 2751.
(9) Doverbratt, I.; Ponou, S.; Lidin, S. *J. Solid State Chem.* **2013**, *197*, 312−316.
(10) (a) Doverbratt, I.; Ponou, S.; Lidin, S.; Fredrickson, D. C. *Inorg. Chem.* **2012**, *51*, 11980−11985. (b) Fredrickson, D. C.; Doverbratt, I.; Ponou, S.; Lidin, S. *Crystals* **2013**, *3*, 504−516.
(11) Doverbratt, I.; Ponou, S.; Zhang, Y.; Lidin, S.; Miller, G. J. *Chem. Mater.* **2015**, *27*, 304.
(12) (a) Pyykkö, P. *Chem. Rev.* **1988**, *88*, 563. (b) Pyykkö, P. *Angew. Chem., Int. Ed.* **2002**, *41*, 1.
(13) Agilent. *CrysAlisPro*, Version 1.171.36.32; Agilent Technologies, UK Ltd: Oxford, England, 2012.
(14) Palatinus, L.; Chapuis, G. *J. Appl. Crystallogr.* **2007**, *40*, 786−790.
(15) *WinXPow 2.10*; Stoe & Cie GmbH: Darmstadt, Germany, 2004.
(16) Petříček, V.; Dušek, M.; Palatinus, L. *Z. Kristallogr. - Cryst. Mater.* **2014**, *229*, 345−352.
(17) Tank, R. W.; Jepsen, O.; Burkhardt, A.; Andersen, O. K.*LMTO-ASA*; Max-Planck-Institut für Festkörperforschung: Stuttgart, Germany, 1998.
(18) von Barth, U.; Hedin, L. *J. Phys. C: Solid State Phys.* **1972**, *5*, 1629.
(19) Jepsen, O.; Andersen, O. K. *Z. Phys. B: Condens. Matter* **1995**, *97*, 35.
(20) Dronskowski, R.; Blochl, P. E. *J. Phys. Chem.* **1993**, *97*, 8617.
(21) Gonze, X. *Z. Kristallogr.* **2005**, *220*, 558.
(22) Gonze, X.; Amadon, B.; Anglade, P. M.; Beuken, J. M.; Bottin, F.; Boulanger, P.; Bruneval, F.; Caliste, D.; Caracas, R.; Côté, M.; Deutsch, T.; Genovese, L.; Ghosez, P.; Giantomassi, M.; Goedecker, S.; Hamann, D. R.; Hermet, P.; Jollet, F.; Jomard, G.; Leroux, S.; Mancini, M.; Mazevet, S.; Oliveira, M. J. T.; Onida, G.; Pouillon, Y.; Rangel, T.; Rignanese, G. M.; Sangalli, D.; Shaltaf, R.; Torrent, M.; Verstraete, M. J.; Zerah, G.; Zwanziger, J. W. *Comput. Phys. Commun.* **2009**, *180*, 2582.
(23) Gonze, X.; Beuken, J. M.; Caracas, R.; Detraux, F.; Fuchs, M.; Rignanese, G. M.; Sindic, L.; Verstraete, M.; Zerah, G.; Jollet, F.; Torrent, M.; Roy, A.; Mikami, M.; Ghosez, P.; Raty, J. Y.; Allan, D. C. *Comput. Mater. Sci.* **2002**, *25*, 478.
(24) Perdew, J. P.; Burke, K.; Ernzerhof, M. *Phys. Rev. Lett.* **1996**, *77*, 3865.
(25) Fuchs, M.; Scheffler, M. *Comput. Phys. Commun.* **1999**, *119*, 67.
(26) Methfessel, M.; Paxton, A. T. *Phys. Rev. B: Condens. Matter Mater. Phys.* **1989**, *40*, 3616.
(27) Häberlen, M.; Glaser, J.; Meyer, H. J. *J. Solid State Chem.* **2005**, *178*, 1478.
(28) Engel, N.; Chabot, B.; Parthe, E. *J. Less-Common Met.* **1984**, *96*, 291−296.
(29) Francisco, M. C.; Malliakas, C. D.; Piccoli, P. M. B.; Gutmann, M. J.; Schultz, A. J.; Kanatzidis, M. G. *J. Am. Chem. Soc.* **2010**, *132*, 8998.
(30) Donohue, J. *The Structures of the Elements*; Wiley: New York, 1974.
(31) Pauling, L. *The Nature of the Chemical Bond*, 2nd ed.; Cornell University Press, 1945.
(32) Siggelkow, L.; Hlukhyy, V.; Fässler, T. F. *J. Solid State Chem.* **2012**, *191*, 76−89.
(33) Venturini, G.; Malaman, B.; Roques, B. *J. Solid State Chem.* **1989**, *79*, 136.
(34) Nesper, R.; Miller, G. J. *J. Alloys Compd.* **1993**, *197*, 109.
(35) Miller, G. J.; Lee, C.-S.; Choe, W. In *Inorganic Chemistry Highlights*; Meyer, G., Naumann, D.; Wesemann, L., Eds.; Wiley-VCH: Weinheim, Germany, 2002.
(36) Nesper, R.; von Schnering, H. G. *J. Solid State Chem.* **1987**, *70*, 48−57.
(37) Mizutani, U.; Inukai, M.; Sato, H.; Zijlstra, E. S. *Chem. Soc. Rev.* **2012**, *41*, 6799−6820.
(38) Miller, G. J. *Eur. J. Inorg. Chem.* **1998**, *5*, 523.

DOI: 10.1021/acs.inorgchem.5b01528
Inorg. Chem. 2015, 54, 9098−9104